BULLETIN OF THE POLISH ACADEMY OF SCIENCES
TECHNICAL SCIENCES, Vol. 68, No. 1, 2020
DOI: 10.24425/bpasts.2020.131842



# Analysis of advanced additive technology in direct metal laser sintering and precision casting method

J. ROBL[1], J. SEDLÁK[1], Z. POKORNÝ[2]*, P. ŇUKSA[3], I. BARÉNYI[4], and J. MAJERÍK[4]

[1] Institute of Manufacturing Technology, University of Technology Brno, Faculty of Mechanical Engineering, Brno, Czech Republic
[2] Department of Mechanical Engineering, University of Defence in Brno, Brno, Czech Republic
[3] Precision casting division, PBS Velká Bíteš a. s., Velká Bíteš, Czech Republic
[4] Department of Engineering, Alexander Dubcek University of Trencin, Faculty of special technology, Trencin, Slovak Republic

**Abstract.** The paper deals with analysis of samples made of Inconel 718 nickel superalloy, produced using direct metal laser sintering (DMLS), known as "sintering", and precision casting technologies. The theoretical part is focused on the characteristics of producing samples of the nickel superalloy by modern additive methods (those for processing metallic materials) and by the conventional technology of precision casting. The practical part involves the investigation of the mechanical properties and texture of the surfaces of the tested samples. A significant part of this study is devoted to analysis of fracture surfaces and EDX experimental testing of TEM lamella by using of electron microscopy methods. The conclusions of this paper include a discussion, evaluation and explanation of both technologies applied on tested samples. Finally, the main benefits of using modern additive technologies in the design and production of heat-resistant components of turbochargers are discussed.

**Key words:** test samples, additive technology, DMLS method, precision casting, Inconel 718.

## 1. Introduction

The speed at which new products can be launched to meet the changing needs of the market is synonymous with the profitability of production. The ability to flexibly react to advancement in science and to adapt to rapid variations in demand are the requirements that have brought about a number of challenges for many engineering companies. Nevertheless, conventional methods employed in the lifecycle of a product are lengthy, and do not align with customer-driven requirements for swift initiation of serial production [1, 2].

Herein, an investigation is conducted into the possibility of using additive technology to produce components for modern turbochargers, such as turbine wheels. On the basis of drawings, reference blanks of Inconel 718 were created. In total, 13 bars were prepared by precision casting for tensile test and another 5 such bars were produced for creep tests, while the DMLS method was applied to fabricate 11 and 6 bars for the same tests, respectively.

For further analysis, casted rods for tensile test at elevated temperature were marked as "L N°" samples, for room temperature – as "L N° – P". For 3D printed samples, the same marking strategy was followed – "T N°" stands for samples for tensile test at elevated temperature, while "T N° – P" for rods dedicated to room temperature tensile test.

The metallography preparation of samples was performed by standard procedures typical for the following evaluation. Firstly, the etching was performed by ferric chloride and nitric acid to reveal the macrostructure of the samples, followed by heat treatment.

After the machining of samples, mechanical tests were performed, i.e. for tensile testing at room temperature (according to EN ISO 6892–1), a tensile test at elevated temperature (according to ISO 6892–2) and a creep test (according to the ČSN ISO 204 procedure). Based on the outputs of these, certain samples underwent transmission and scanning electron microscopy to examine fractured areas and facilitate EDX analysis of TEM lamellas [2, 3].

## 2. Experimental work

The used additive technology is a method for material joining that creates spatial objects layer upon layer based on 3D model data. This is different from conventional technologies in which the shape of a product is formed through removing material or transforming existing geometry. One additive method that meets prerequisites for producing heat-resistant components is direct metal laser sintering (DMLS). This technology is classified by ISO 52900:2015 as one of several powder bed fusion technologies. No complete fusion of particulate matter occurs in DMLS. Instead, the principle of the process involves heating metallic powder molecules at high temperatures, thereby connecting them at a molecular level. Energy is transferred to the point of sintering by means of a laser beam, which is employed to heat the molecules of metallic powder. Notably, the melting temperature of the processed material is never exceeded. This metallic powder is possible to modify by using diffusion technologies [4–8].

*e-mail: zdenek.pokorny@unob.cz

Manuscript submitted 2019-07-03, revised 2019-10-01, initially accepted for publication 2019-10-18, published in February 2020

A standardized process of the PBS Velká Bíteš, a. s. company was utilized to prepare the cast test bars. Further details are provided below. The additive method applied herein required creating a suitable model in a 3D environment. Test rods were modelled according to supplied drawing documentation, with addition of an allowance for machining and centring pits.

All the samples were heat treated according to AMS 5664 standard.

Moreover, for machining purposes, the diameter of the component was enlarged by 1.2 mm to enable a presumed three passes of a turning tool with a cutting edge of radius 0.2 mm. Images of the test bars are shown in Fig. 1 and Fig. 2.

Inconel 718 3D printing parameters are delivered as part of an EOS M290 printer software package which encompasses complete set-up of the entire device. The output of the laser beam varies according to the printing area during the printing process. For the given samples, the specific power output ranged from 27 to 370 W. A 0.08 diameter of beam resulted in a "fusion field" of diameter 0.15 to 0.2 mm [9].

Standardized blanks of the PBS Velká Bíteš, a. s. company, with the designation "Type 1 – 816794" for the creep test and "Type 3 – 816788" for the tensile test, were employed to make test bars by precision casting. The first type was cast in shell moulds made up to 7 pieces per gating system, with a total weight of 3 kg. In the case of the bars for the tensile test, 9 pieces per gating system were utilized with a total weight of 6 kg. Casting was carried out in an ISK5 two-chamber vacuum furnace; the charge consisted of 100% virgin Inconel 718 material. The blanks were separated from the gating system by a circular saw. Detailed casting parameters are given in Table 1 [1].

Table 1
Casting parameters

| | Creep test | Tensile test |
|---|---|---|
| **Sample identification** | **Type 1** | **Type 3** |
| Model no. | 816794 | 816788 |
| Weight | 0.075 kg | 0.115 kg |
| Pieces per gating system | 7 pcs | 9 pcs |
| Total weight | 3 kg | 6 kg |
| Shell temperature | 1,050°C | 1,050°C |
| Casting temperature | 1,362°C | 1,360°C |
| Vacuum | $4 \cdot 10^{-2}$ mbar | $4 \cdot 10^{-2}$ mbar |

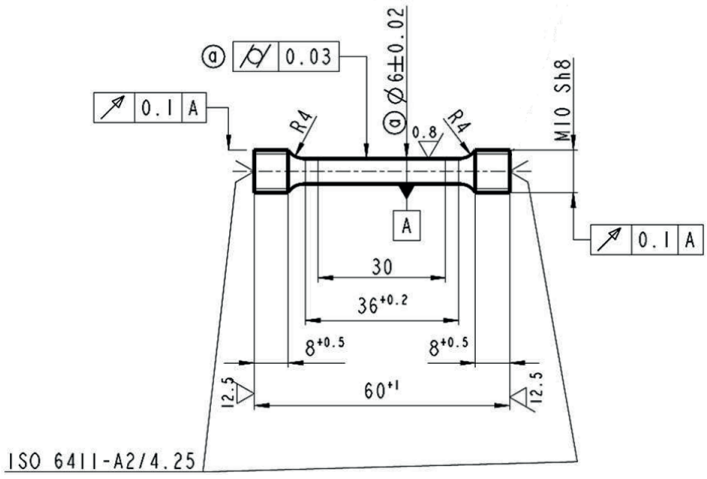


Fig. 1. Dimensions of creep test rod

Fig. 3. Blank bar for the tensile test

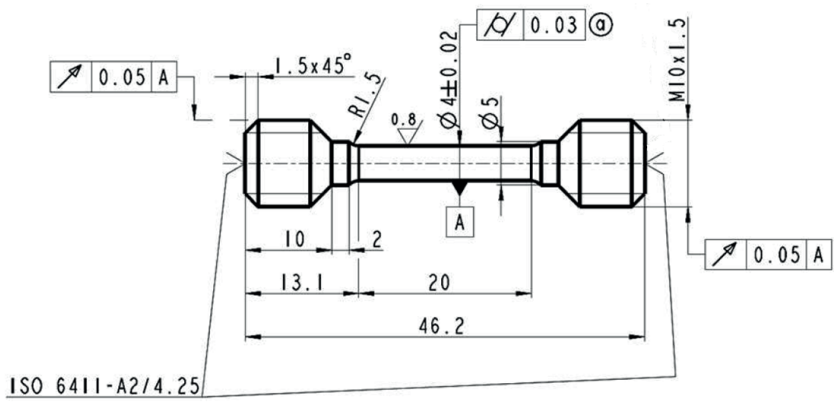


Fig. 2. Dimensions of tensile test rod

Fig. 4. Blank bar for the creep test

Two heat-treated printed samples for the tensile test were randomly selected to evaluate the material structure. One of the blanks was left without any modification (sample A), while the second was blasted (sample B). The areas comprised 3 sections (Fig. 5) – area 1, which constituted the largest diameter of the sample, whereas area 2 pertained to the smallest diameter, and the radius of the last area (3) was created by increasing the diameter of the sintered geometry of the previous layer.

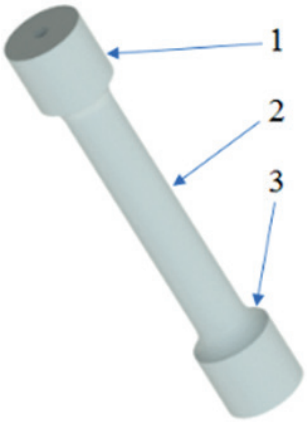


Fig. 5. Evaluated areas on the sintered samples

These areas were cleaned by isopropyl alcohol and the magnification 20× lens was used to evaluate them. The process was performed on all the selected areas. Surface texture analysis was also carried out on Taylor Hobson Talysurf CCI Lite instrument.

The mechanical properties of the samples by testing their tensility were evaluated at room temperature according to EN ISO 6892–1, and at elevated temperatures according to ISO EN 6892 2. Standardized test bars were performed according to drawings by PBS Velká Bíteš, a. s. [2, 12].

An electron microscope was focused on the fracture areas of the sintered and cast parts and was performed after tensile tests on the selected samples. The machined samples were cleaned in an ultrasonic cleaner and were studied on a TESCAN LYRA 3 scanning microscope [14–16]. In all cases, a secondary SE electron detector was used, and the samples were studied at 35×, 100× and 500× magnification.

The TEM lamella for EDX analysis was made from the threaded portion of the L3 and T1 sample (after the tensile test at elevated temperature had been conducted) in order to carry out EDX analysis and determine the potential causes of poor mechanical properties of the cast material. Preparation of the lamella in the Helios microscope involved several technological steps. Initially, a rectangular protective platinum layer of 2×10 µm and 100 nm in thickness was deposited by electron beam-induced deposition (EBID), followed by focused ion beam-induced deposition (FIBID) of 2,000 nm; both deposition layers are visible in Fig. 6a. The next step was to form a three-sided trench around the platinum layer to cut the L-shaped lamella, as shown in Fig. 6b. Afterwards, a nano-manipulator was attached to the platinum layer to facilitate removal of the lamella from the samples. The lamella was fixed to a copper holder by platinum deposition. The last step of the preparation was to thin the lamella from 2 µm to the final value of 100 nm, as displayed in Fig. 6c [14, 17–19].

The prepared Inconel 718 lamella was placed in a special holder for energy dispersive X-ray spectroscopy (EDX). EDX measurements were carried out on a TITAN transmission elec-

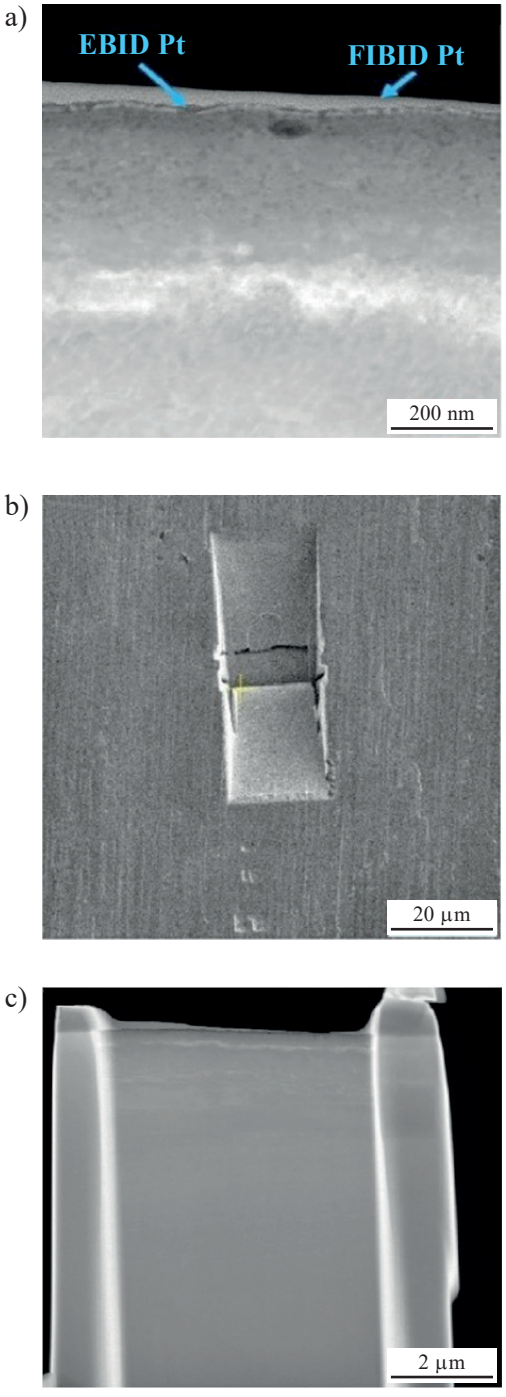


Fig. 6. Preparation of TEM lamella: a) deposition of platinum by EBID and FIBID; b) three-sided trench around the platinum layer; c) eventual thinned lamella

tron microscope set to scan mode. The X-ray signal generated by the impact of high-energy electrons (300 kV) was analysed by the detector. The obtained data was evaluated by Velox software (version 2.3).

## 3. Results

Surface texture analysis outputs from Taylor Hobson Talysurf CCI Lite are shown as 3D models of the resultant textures in Figs. 7–12 [10, 11].

It was not possible to analyse height parameters according to ČSN ISO 4288:1999 due to large differences in roughness of the samples. For this reason, it was necessary to evaluate parameters via a touch probe method (with a Mitutoyo Surftest SJ-301). As a consequence of constraints inherent to the latter method, roughness was only calculated for areas 1 and 2. The outputs of this method are detailed in Table 2 [10, 11].

Table 2
Surface roughness of sintered samples

| | Quantity [µm] | Sample A | Sample B |
|---|---|---|---|
| Area 1 | Ra | 3.68 | 3.35 |
| Area 1 | Rz | 22.44 | 19.26 |
| Area 2 | Ra | 4.08 | 3.84 |
| Area 2 | Rz | 19.64 | 23.77 |

Sample A – heat-treated only

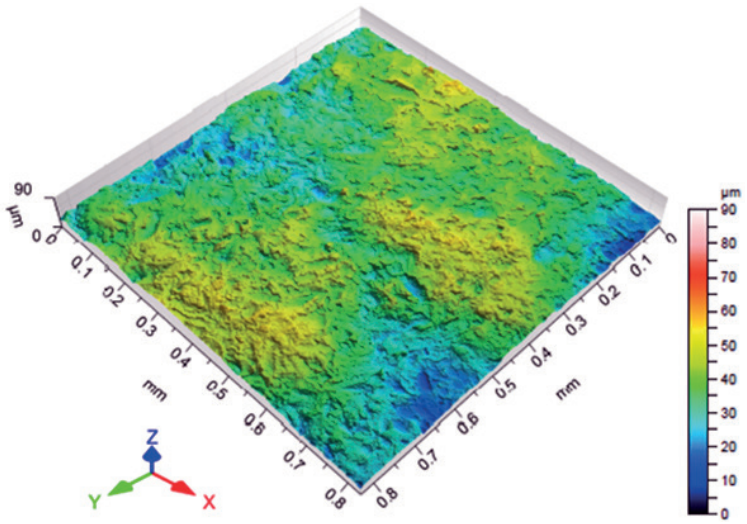


Fig. 7. Model of surface texture (1)

Sample B – blasted

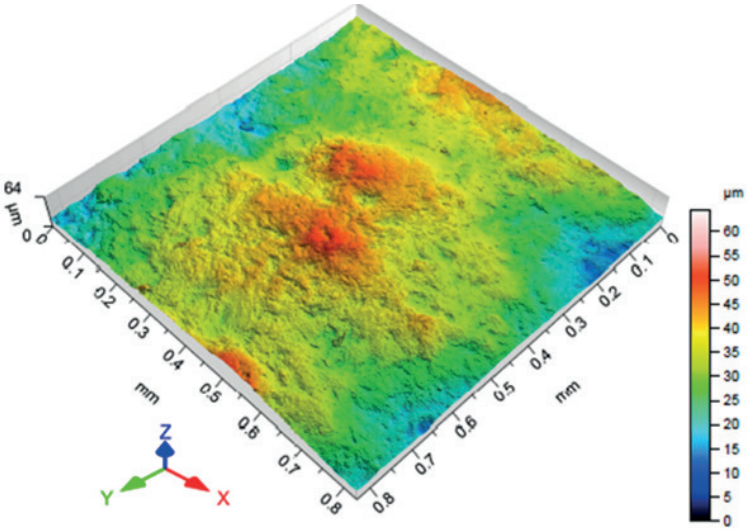


Fig. 8. Model of surface texture (1)

Sample A – heat-treated only

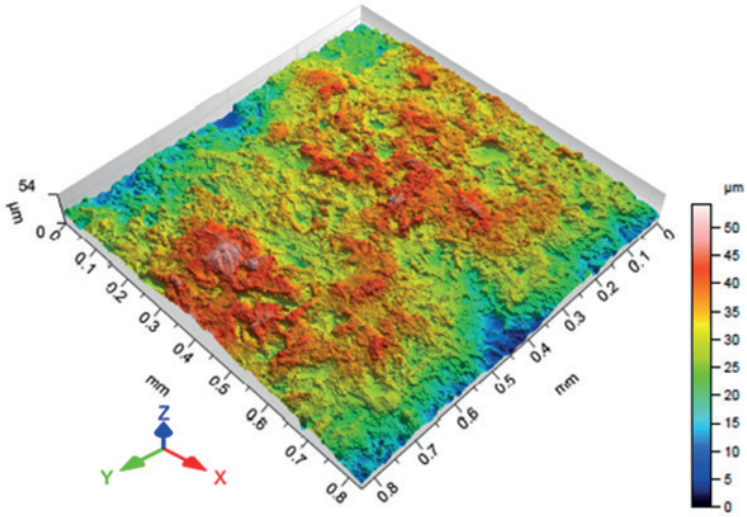


Fig. 9. Model of surface texture (2)

Sample B – blasted

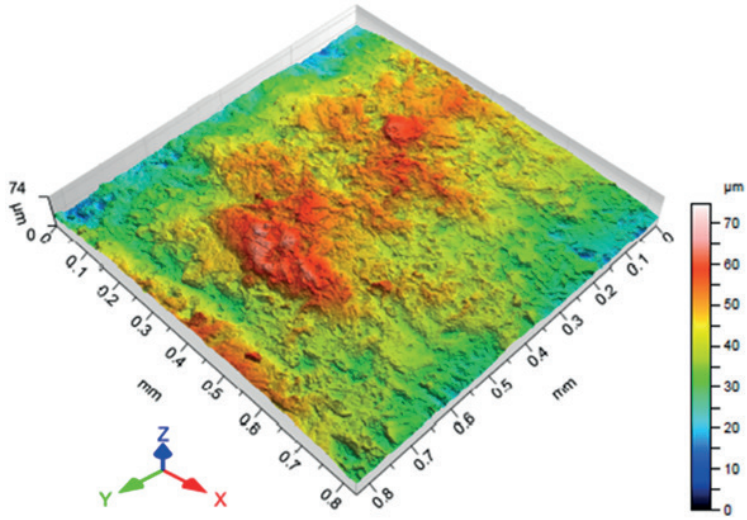


Fig. 10. Model of surface texture (2)

Sample A – heat-treated only

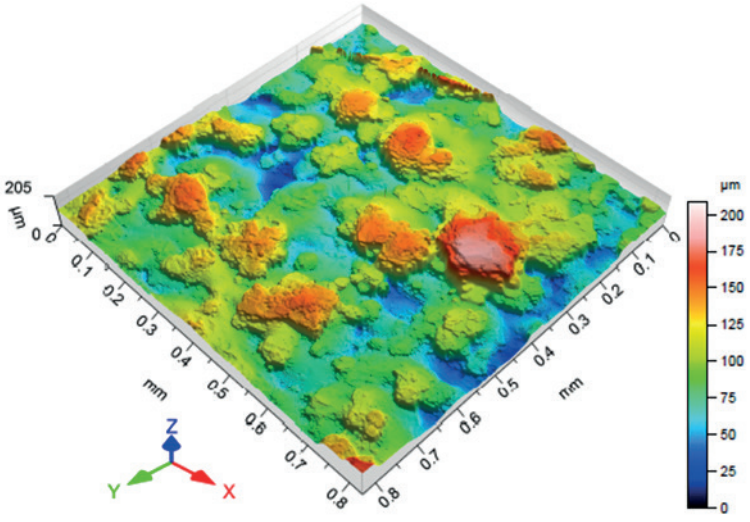


Fig. 11. Model of surface texture (3)

Sample B – blasted

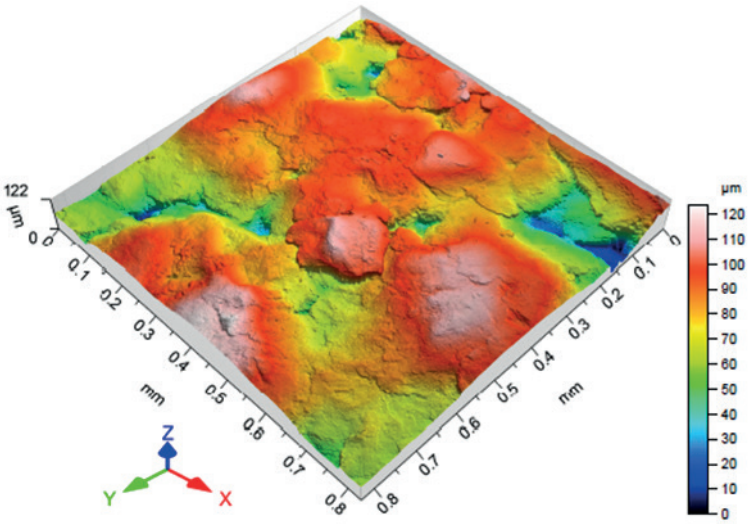


Fig. 12. Model of surface texture (3)

It was not possible to analyse height parameters according to ČSN ISO 4288:1999 due to large differences in roughness of the samples. For this reason, it was necessary to evaluate parameters via a touch probe method (with a Mitutoyo Surftest SJ-301). As a consequence of constraints inherent to the latter method, roughness was only calculated for areas 1 and 2. The outputs of this method are detailed in Table 2.

Tensile tests at 600°C was chosen to examine mechanical properties at the elevated temperatures. Such testing of 6 sintered and 7 cast samples was performed by TÜV NORD Czech, s. r. o.; the results are given in Table 3 an Table 4 [2].

Table 3
Outputs of tensile tests on cast samples at an elevated temperature

| Sample identification | Yield strength $R_{p\,0.2}$ [MPa] | Tensile limit $R_m$ [MPa] | Contraction $Z$ [%] | Ductility $A_5$ [%] |
|---|---|---|---|---|
| L1 | 733.0 | 838.0 | 15.1 | 5.5 |
| L2 | 742.5 | 880.5 | 11.0 | 8.4 |
| L3 | 770.1 | 888.1 | 16.4 | 8.1 |
| L4 | 708.8 | 894.5 | 12.3 | 11.7 |
| L5 | 721.7 | 897.5 | 17.2 | 8.9 |
| L6 | 728.8 | 848.4 | 16.6 | 7.1 |
| L7 | 737.5 | 896.1 | 9.1 | 8.2 |

Tensile tests at room temperature were carried out in the laboratory of the Precision Casting Division at PBS Velká Bíteš, a. s. For this purpose, a total of 5 sintered and 7 cast test bars were prepared. The results are given in Table 5 and Table 6 [12].

Table 4
Outputs of tensile tests on sintered samples at elevated temperature

| Sample identification | Yield strength $R_{p\,0.2}$ [MPa] | Tensile limit $R_m$ [MPa] | Contraction $Z$ [%] | Ductility $A_5$ [%] |
|---|---|---|---|---|
| T1 | 1061.3 | 1237.7 | 28.2 | 11.8 |
| T2 | 1061.6 | 1234.6 | 30.6 | 13.9 |
| T3 | 1060.1 | 1232.6 | 29.6 | 14.4 |
| T4 | 1051.6 | 1224.7 | 31.4 | 16.7 |
| T5 | 1051.8 | 1237.7 | 28.8 | 16.3 |
| T6 | 1040.8 | 1245.6 | 24.1 | 12.4 |

Fundamental differences were revealed during mechanical tests. The most obvious was in the outputs of the tensile test

Table 5
Outputs of tensile tests on cast samples at room temperature

| Sample identification | Yield strength $R_{p\,0.2}$ [MPa] | Tensile limit $R_m$ [MPa] | Ductility $A_5$ [%] |
|---|---|---|---|
| L1-P | 865 | 1046 | 4.4 |
| L2-P | 866 | 1076 | 7.0 |
| L3-P | 835 | 1047 | 4.7 |
| L4-P | 881 | 1036 | 3.3 |
| L5-P | 870 | 1083 | 7.7 |

Table 6
Outputs of tensile tests on sintered samples at room temperature

| Sample identification | Yield strength $R_{p\,0.2}$ [MPa] | Tensile limit $R_m$ [MPa] | Ductility $A_5$ [%] |
|---|---|---|---|
| T1-P | 1076 | 1392 | 20.5 |
| T2-P | 1144 | 1388 | 19.9 |
| T3-P | 1173 | 1389 | 18.1 |
| T4-P | 1100 | 1383 | 18.3 |
| T5-P | 1213 | 1391 | 19.0 |

at elevated temperature, where the sintered material exhibited strength limits above the 1200 MPa limit. In contrast, the cast samples demonstrated strength limits of up to 900 MPa.

The final texture of the printed part was greatly affected by its external geometry. For the cylindrical surfaces (areas 1 and 2), the average arithmetic deviation of the profile was approximately above the value Ra = 3.8 μm. Such roughness does not meet modern surface quality requirements for parts manufactured by precision casting technology; usually, roughness does not exceed the value Ra = 3.2 μm. For this reason, the components produced by the DMLS additive method would appear to be unsuitable for heat resistant applications without undergoing subsequent surface treatment. Poor surface roughness could be improved by incorporating stages of machining or tumbling into the technological process of printed parts.

Selected outputs from mechanical properties are shown in Fig. 13 and Fig. 14. The AMS 5663 M standard was applied to

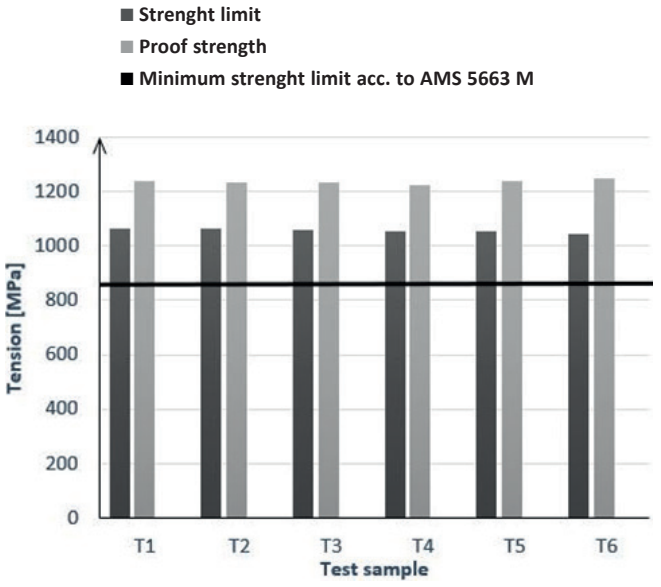


Fig. 13. Mechanical properties of material processed by DMLS at 600°C

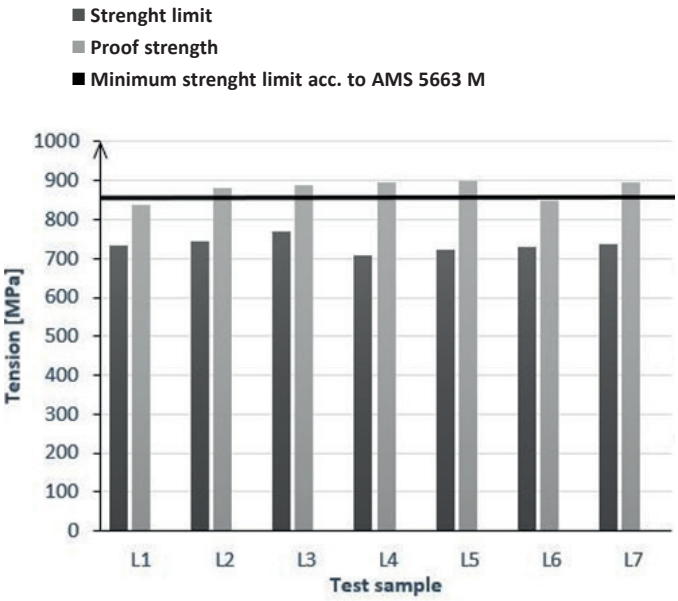


Fig. 14. Mechanical properties of material processed by precision casting at 600°C

evaluate the Inconel 718 material. Notably, slight differences were discerned between the process employed herein and the AMS 5663 M standard. Indeed, the tendency is to utilize imperial units in the AMS (aerospace material specification) standard. After converting these units into the SI system, slight differences between the procedures were visible. This was especially the case for mechanical tests at the elevated temperature (600°C), since the AMS 5663 M standard recorded the value of 1.200°F (i.e. 649°C). For these and other reasons, the limits set by the AMS 5663 M standard should largely be considered as indicative [1, 9, 13].

Significant differences were also observed for ductility and mechanical properties at room temperature. In this context, 5 out of 6 samples met limits set by the AMS 5663 M standard, whereas none of the cast samples reached values for expected limits. A similar trend was observed for contraction values, in relation to which all the printed samples exceeded the limit by more than 30%, while the requirement was only met in 4 instances of the cast samples [13].

Such significant differences in the mechanical properties of the cast material might have been caused by adverse conditions of heat treatment. The values required by EOS for the heat treatment of DMLS parts (AMS 5664) differ slightly from those applicable for cast materials according to AMS 5663 M. Specifically, the maximum temperature was increased from 1010°C to 1065°C for dissolving annealing, while the duration of precipitation at 760°C is extended by 2 hours [1, 9, 13].

After analysis of the heat treatment, a slight deviation from the AMS 5664 standard was additionally found. In summary, it differed from AMS 5663 M by 55°C for dissolving annealing, the time at 760°C was extended by 2 hours and the duration at 650°C was also extended by 2 hours [1, 9, 13].

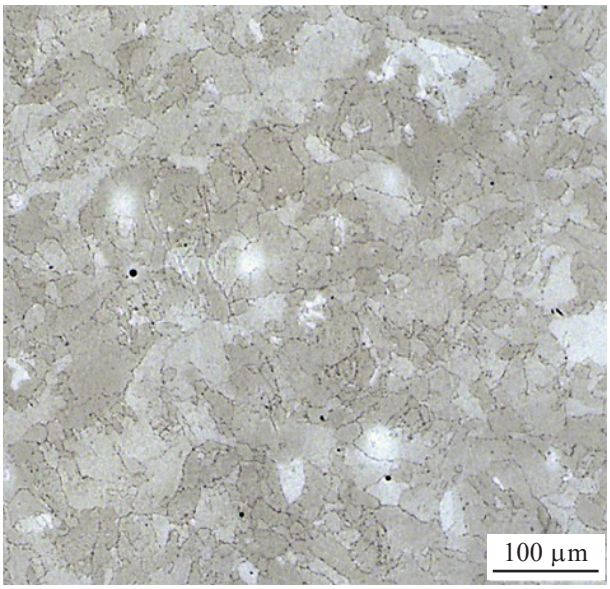


Fig. 15. Microstructure of sample T1, 10× magnification

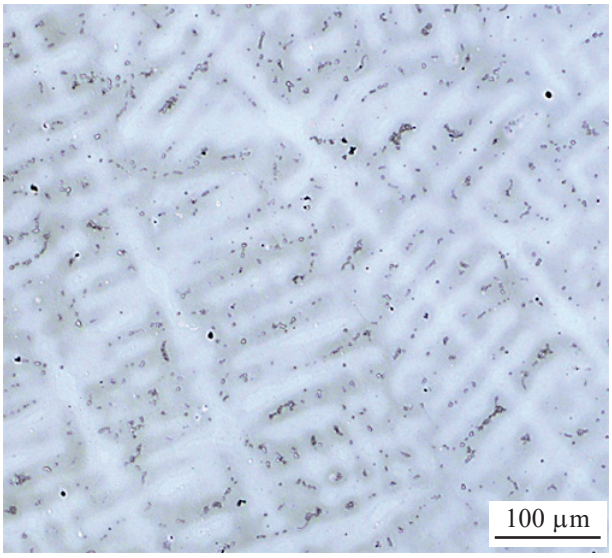


Fig. 16. Microstructure of sample L3, 10× magnification

Creep test was performed at 870°C with initial load of 353 MPa. Unfortunately, these parameters were shown as excessive and all the samples failed after starting the test.

A more detailed experiment would be required to determine if these differences in heat treatment were caused by poor mechanical properties of the cast samples.

In relation to the cast samples, fractures propagated mainly along grain boundaries and primary dendrites (shown by arrow in Fig. 17).

However, the sintered material exhibited fractures propagated through the fine-grained structure (the microstructure of samples T1 and L3 is shown in Fig. 15 and Fig. 16) [1].

Figure 17 to 22 illustrate the fracture surfaces of samples T1 and L3 [14, 15].

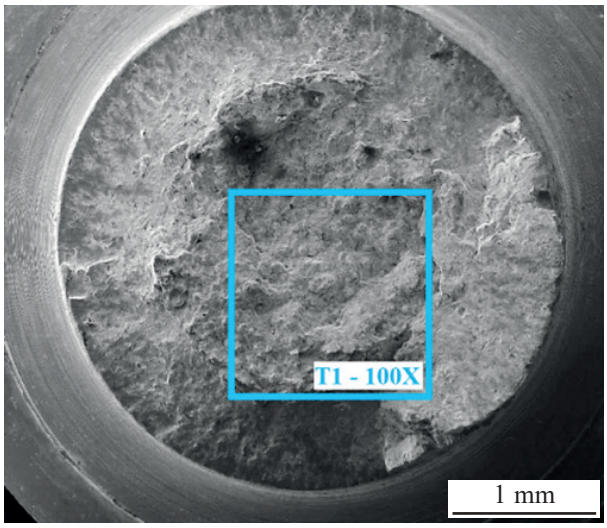


Fig. 17. Sample T1, 35× magnification

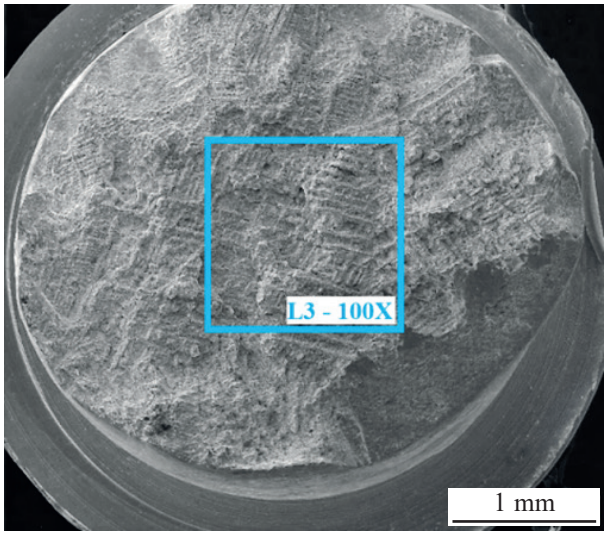


Fig. 18. Sample L3, 35× magnification

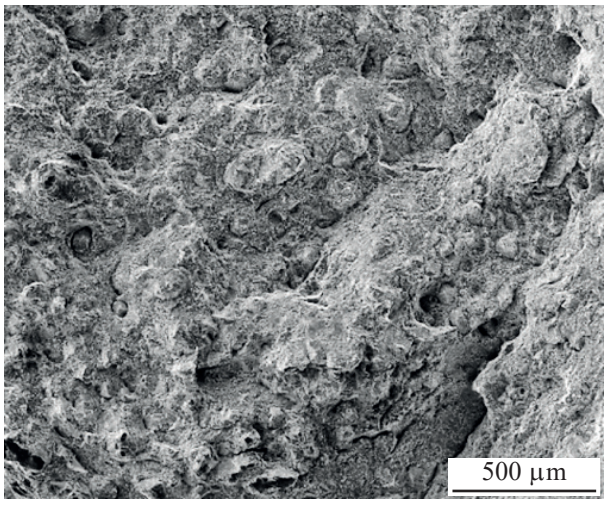


Fig. 19. Sample T1, 100× magnification

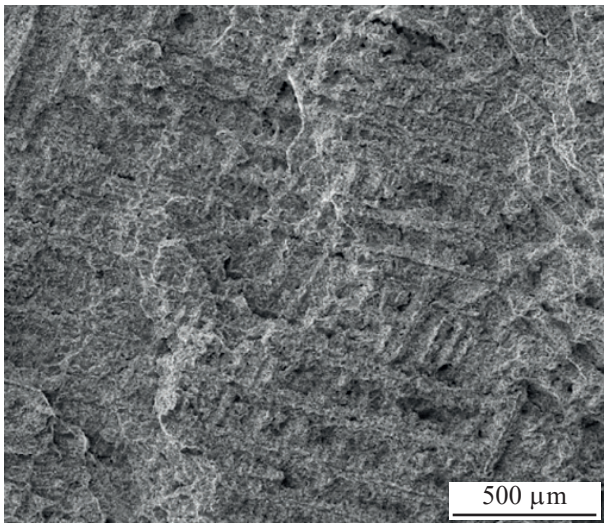


Fig. 20. Sample L3, 100× magnification

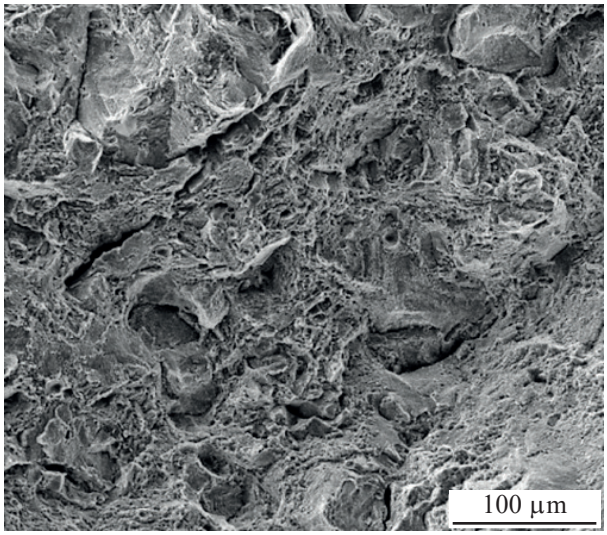


Fig. 21. Sample T1, 500× magnification

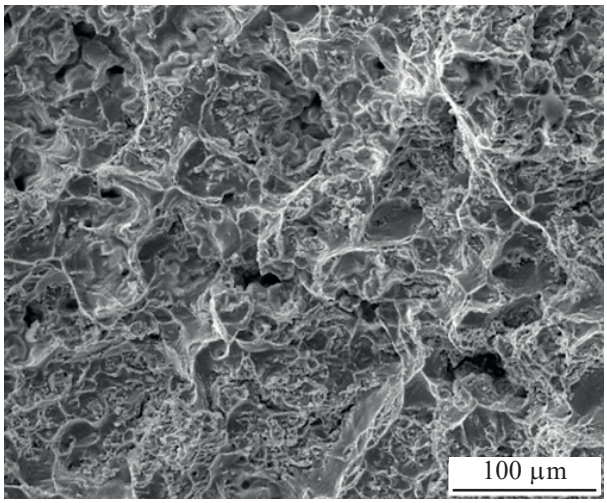


Fig. 22. Sample L3, 500× magnification

In order to perform detailed EDX analysis, first it was necessary to make a preliminary scan of a large area of the prepared lamella (Fig. 23) [14, 17–19].

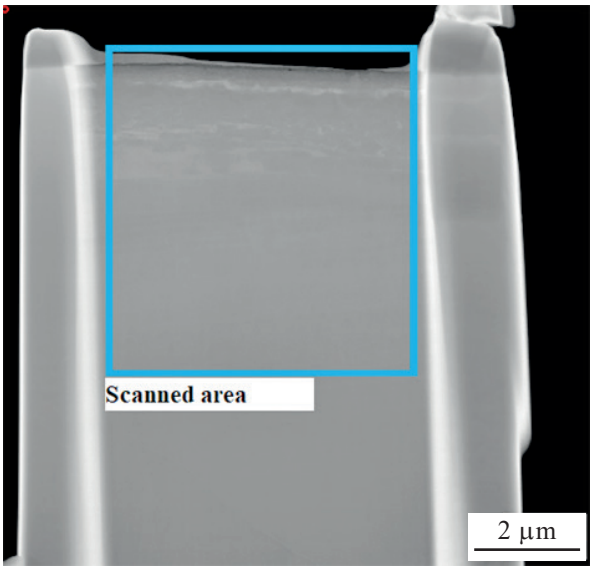


Fig. 23. Area of the first EDX scan of the TEM lamella

Next step involved scanning a smaller area (Fig. 24).

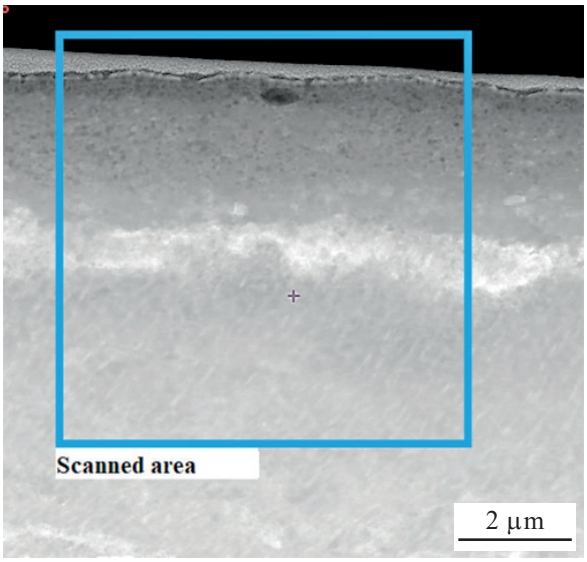


Fig. 24. Area of the second EDX scan of the TEM lamella

The last site to undergo EDX analysis to gauge the chemical composition of the cast samples was the area of the grain boundaries at the bottom of the lamella (Fig. 25).

EDX analysis revealed that the precision casting material showed significant reduction in the concentration of chromium and iron at the grain boundaries, which correlates with an inverse rise in niobium and titanium. No additional major

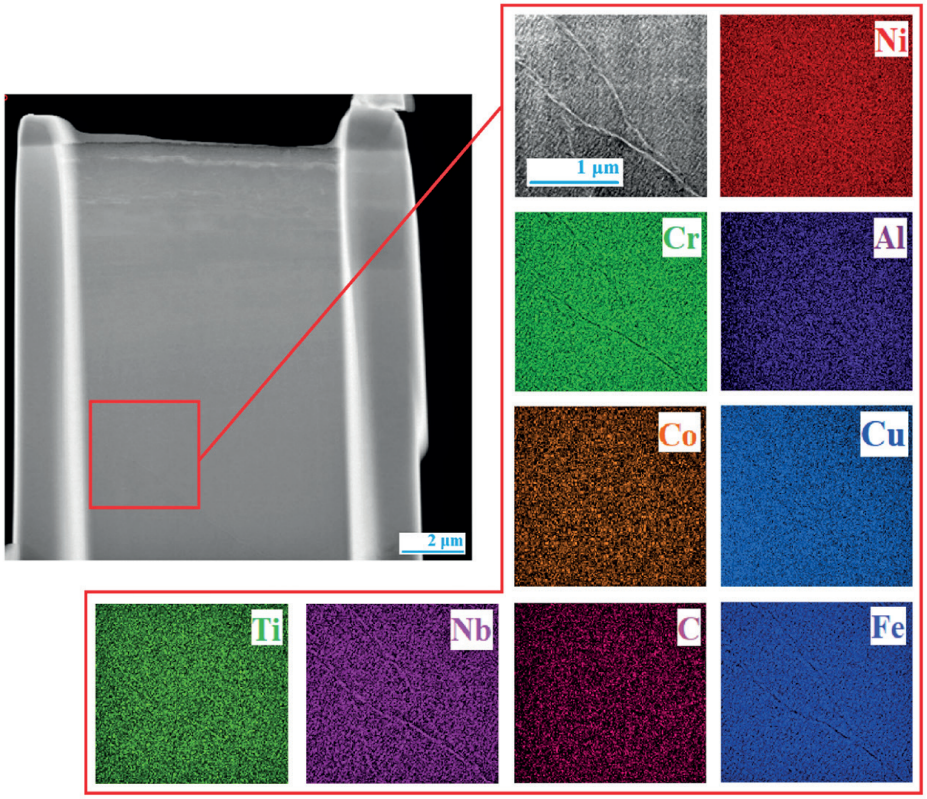


Fig. 25. EDX scan of the area of grain boundaries with colour-coded weight fractions of selected elements complemented by a TEM image in HAADF mode

variation in the concentration of other elements was observed in the scanned area [20, 21].

The next step was lamella analysis performed from a printed sample. Detailed scan of the lamella revealed fainter lines on the printed material, which were visible in the image taken in HAADF mode. These lines demarked where there was a rise in the level of niobium and a drop in iron and chromium, although to a much lesser extent than at the grain boundaries of the cast material. This would suggest that observed lines constitute the boundary of gradual solidification of the melting pool. This theory is also backed up by the direction and inclination of the lines, the average spacing of which is approximately 1 micrometre [1].

The results of the EDX scan of the printed material show that there are far fewer areas with reduced concentration in iron and chrome. The concentration of all elements in printed sample seems much more uniform with steady distribution, without major fluctuations. In comparison to the cast specimen, these areas are much smaller and not nearly as extensive [1].

## 4. Conclusions

The main goal of the paper was to provide insight into the emerging field of metallic 3D printing, focusing on the suitability of this technology for heat-resistant applications. In recent years, the rapid development of additive technology has resulted in the appearance of new, advanced materials, including the nickel superalloy Inconel 718. Such swift development has created new opportunities for additive technology in areas previously dominated by conventional methods. In order to determine the current state and properties of such materials, the authors devised an experiment comprising a series of tests to explore the possible applicability of additive DMLS technology and compare it with the precision casting method.

- The following conclusions are based on results from the experimental part of this study:
- When creating a model for 3D printing, it is necessary to take into account overmelt of the material into the unsintered powder of the previous layer, which results in deterioration of the texture of the outer geometry of the given part.
- Printed samples possess greater surface roughness and more surface defects than semi-finished products prepared by precision casting.
- For components made by the additive DMLS method to be potentially suited to heat-resistant applications, it is necessary to incorporate a stage of machining or tumbling into the manufacturing process.
- The material created herein by the additive DMLS method exhibited significantly higher mechanical properties than the material processed via precision casting.
- The fracture surfaces of the samples from the two technologies differed mainly in the propagation of the fracture crack. In the cast material, the fracture crack followed the

dendrite and grain boundaries, whereas the printed material demonstrated a fracture crack that passed through the finer structure.

Additive technology is a rapidly evolving area with the potential to influence most industries in the future. In recent years, the number of workable materials has expanded to comprise several new titanium and nickel-based superalloys. Therefore, it should be possible to extend the range of materials applicable for such additive technology even further, e.g. to incorporate nickel superalloys like Inconel 713 or Mar M 247. To this end, it shall be necessary to develop new sintering parameters and evolve the given technologies in order to explore the possibility of applying such materials industrially.

As for the applicability of the DMLS method for heat-resistant applications, the authors conclude that such components are suitable for further testing with the intention of real-world utilization. This assertion is supported by the high values for mechanical properties that meet the requirements of the AMS 5663 M standard. However, for production of a functional heat-resistant component, it would be advisable to consider adding a finishing stage of machining or tumbling in the process.

**Acknowledgements.** This article was supported by the Precision Casting Division of PBS Velká Bíteš, a. s. and by specific research 2019, with the grant "Research on perspective production technologies", FSI-S-19–6014. The work also benefitted from the support of CEITEC Nano Research Infrastructure (ID LM2015041, MEYS CR, 2016–2019) at CEITEC Brno University of Technology and by a research Project for the Development of Technologies, Design of Firearms, Ammunition, Instrumentation, Engineering of Materials and Military Infrastructure "VÝZBROJ (DZRO K201)". This work was also supported by the Slovak Research and Development Agency under the contract No. APVV-15–0710.

## References

[1] R. Walzak, "Inkjet 3D printing – towards new micromachning tool for MEMS fabrication", *Bull. Pol. Ac.: Tech*. 54(2), 2018.
[2] ČSN EN ISO 6892–2 Metallic materials – Tensile testing – Part 2: Method of test at elevated temperature.
[3] Kovové materiály – Metallic materials – Uniaxial creep testing in tension – Method of test.
[4] R. Castells, "Element", 2016, [Online].
[5] Z. Pokorný, O. Barborák, and V. Hrubý, "Characteristics of plasma nitrided layers in deep holes", *Kovové Materiály – Metallic Materials* 50(3), 209–212, 2012.
[6] C. K. Chua, K. F. Leong, C. S. Lim, *Rapid Prototyping: Principles and Applications*, 3rd ed., World Scientific, Singapore, 2010 DOI: 10.1142/6665
[7] M. Drapela, "Modul Rapid Prototyping", [Online].
[8] J. Sedlák, M. Ptáčková, J. Nejedlý, M. Madaj, J. Dvořáček, J. Zouhar, M. Píška, and L. Rozkošný, "Material analysis of titanium alloy produced by Direct Metal Laser Sintering", *International Journal of Metalcasting* 7(2), 43–50, 2013.
[9] R. Kosturek, M.Wachowski, L. Śnieżek, and M. Gloc, „The influence of the post-weld heat treatment on the microstructure of inconel 625/carbon steel bimetal joint obtained by explosive welding". Metals 9(2), 2019.
[10] R. Jankových, M. Hammer, and M. Harčarík, "Bore quality of shotgun barrel blanks", *MM Science Journal*, 728–730, 2015.
[11] J. Majerník and M. Podařil, "Evaluation of the temperature distribution of a die casting mold of X38CrMoV5_1 steel", *Archives of Foundry Engineering*, 2(19), 107–112, 2019.
[12] D. Dobrocký, Z. Pokorný, Z. Studený, and M. Šurlaková, "Influeance of the carbonitriding to change the surface topography of 16MnCr5 steel", *METAL 2017 – 26th International Conference on Metallurgy and Materials*, 2017, 1085–1091
[13] ČSN EN ISO 6892–1 Kovové materiály – Zkoušení tahem – Část 1: Zkušební metoda za pokojové teploty / Metallic materials – Tensile testing – Part 1: Method of test at room temperature.
[14] Nickel Alloy, Corrosion and Heat-Resistant, Bars, Forgings, and Rings 52.5Ni – 19Cr – 3.0Mo – 5.1Cb (Nb) – 0.90Ti – 0.50Al – 18Fe Consumable Electrode or Vacuum Induction Melted 1775°F (968°C) Solution and Precipitation Heat Treated.
[15] CEITEC: Research Centre, Brno: CEITEC, 2018. [Online]
[16] J. Sedlák, D. Říčan, M. Píška, and L. Rozkosny, "Study of materials produced by powder metallurgy using classical and modern additive laser technology", *Procedia Engineering* 100, 1232–1241, 2015.
[17] J. Sedlák, T. Drábek, K. Mouralová, J. Chladil, and K. Kouřil, "Machining issues of titanium alloys", *International Journal of Matelacasting* 9(2), 41–50, 2015.
[18] K. Mouralová, J. Kovář, I. Klakurková, J. Bednář, L. Beneš, and R. Záhradníček, "Analysis of surface morphology and topography for pure aluminium machined using WEDM", *Journal of International Measurement Confererederation* 114, 169–176.
[19] K. Mouralová, J. Kovář, L. Klakurková, T. Prokeš, and M. Horynová, "Comparison of morphology and topography of surfaces of WEDM machined structural materials", *Journal of International Measurement Confererederation* 104, 12–20, 2017.
[20] K. Mouralová, R. Matoušek, J. Kovář, J. Mach, L. Klakurková, and J. Bednář, "Analyzing the surface layer after WEDM depending on the parameters of a machine for the 16MnCr5 steel", *Journal of International Measurement Confererederation*, 94, 771–779, 2016.
[21] Z. Pokorný, D. Dobrocký, J. Kadlec, and Z. Studený, "Influence of alloying elements on gas nitriding process of high stressed machine parts of weapons", *Kovové Materiály – Metallic Materials* 56(2), 97–103, 2018.